Detection of EDM Defects Under Monju Support Plate Using Experimental Data from Remote Field Eddy Current Probes and a Multi-frequency Algorithm

Ovidiu MIHALACHE, Japan Atomic Energy Agency, FBR Research Center Non-Member
Toshihiko YAMAGUCHI, Japan Atomic Energy Agency, FBR Research Center Non-Member
Masashi UEDA, Japan Atomic Energy Agency, FBR Research Center Non-Member
Takuya YAMASHITA, Japan Atomic Energy Agency, FBR Research Center Member

This paper describes detection of electro-discharged machine (EDM) defects in magnetic steam generator (SG) tubes of Monju fast breeder reactor (FBR). The EDM defects are located under support plate (SP), on the outer tube surface and they are detected by a remote field eddy current probe. Using the experimental measurements and a multi frequency algorithm, the defect signal can be extracted from the SP signal. The parameters of the multi-frequency algorithm were calculated by comparing SP measurements with two-dimensional finite element simulations (FEM).

Keywords: Remote Field Eddy Current, EDM Outer Defect, Monju FBR Support Plate, Steam Generator

1 Introduction

In Monju FBR, the evaporator SG tubes are made of 2.25Cr-1.0Mo allow. Due to their ferromagnetic properties, detection of defects located on the outer tube surface is performed using the principles of the remote field eddy current technique (RFEC) [1]. The RFEC method relies on the propagation of the electromagnetic field from the excitation coil system through the tube wall and then along tube length and back trough tube wall to the detection coil system which is located in a remote field area, 2 or 3 tube diameters far from the excitation zone. The detection coil system consists in two circular bobbin coils, differentially connected.

In the in-service inspection of Monju SG tubes it is very important to be able to detect defects before they penetrate the tube wall. SG tube wall is the only barrier between the sodium flow, outside of SG tubes, and steam water inside of SG tubes. Since, SG tubes are supported using SP, it is expected that defects have a higher probability to appear near and under SP. The geometry of Monju SP is presented in Figure 1. It consists in two plates which encircle the tube, 60 mm far from each other and another horizontal plate, 10 mm thick that connects the two vertical plates.

Ovidiu MIHALACHE, Japan Atomic Energy Agency, Fast Breeder Reactor Research and Development Center, 1 Shiraki, Tsuruga-shi, Fukui-ken, 919-1279, Tel: 0770 39 1031 (ext 5211), email: mihalache.ovidiu@jaea.go.jp

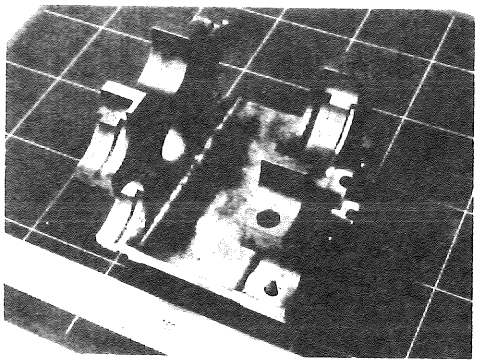

Fig. 1 Geometry of Monju support plate.

The SG tube is closely connected with one encircling plate of the SP using a ring made of austenitic stainless steel. For the second encircling plate, there is a 2-3 mm gap between SP and SG tube. SG tube can move free in this gap touching or not the SP. The SP is made on the same material as the SG tube. Due to the friction between SG tube and SP, by the thermal expansion of SG tube, defects can appear under SP and their signal is masked by SP plate signal.

In the present paper is presented a method to extract the defect signal masked by the SP using a multi-frequency algorithm. The parameters of the algorithm are founded out by accurately calibrating finite element simulations of Monju SP with experimental measurements. The algorithm is then applied to real experimental measurements of signal from defects under SP in SG tubes. The SP signal is suppressed to reveal the signal from the defect under SP.

2. Experimental Measurements of EDM Defects under Monju Support Plate

An EDM defect was machined in a SG tube similar with Monju FBR SG tubes. The defect is on the outer tube surface (OD) full circumferentially, 5 mm wide and 50% from the tube wall thickness (see Figure 2). Tube thickness is 4.1 mm. The defect can be located under SP in the positions indicated in Figure 3.

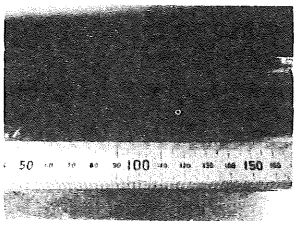

Fig 2. OD 50% groove, 5 mm wide in SG tube

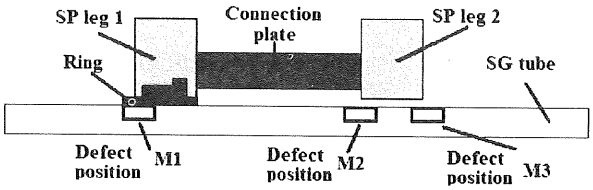

Fig 3. Position of defects near SP: M1, M2 and M3.

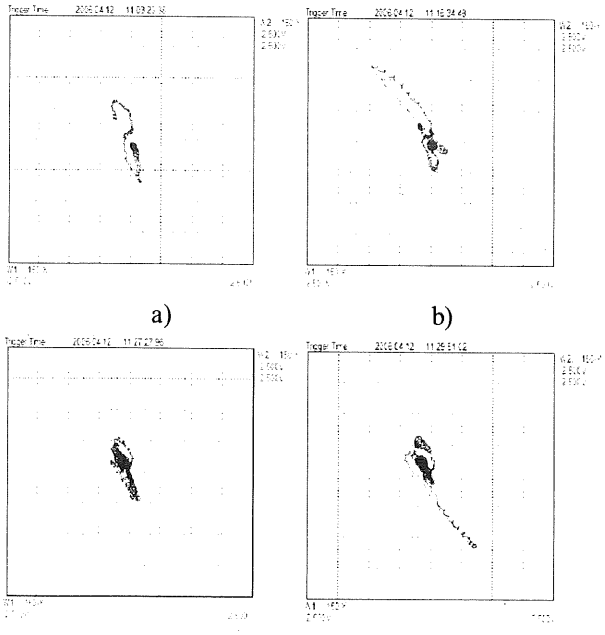

Fig 4. Experimental measurements of the SP signal and defect under SP: a) SP signal only;
SP and OD50% groove in position: b) M1; b) M2; c) M3.

Position M1 corresponds to the zone under first leg of SP, near ring. M2 and M3 locations are under second SP leg, left-side and right-side respectively.

The defect signal, when defect is under SP, was measured using a double RFEC system, which has two excitation modules, one in front and the other one in the back of the detection system, at equal distances. The detection system consists in two bobbin circumferential coil oppositely connected.

Figure 4a presents the Lissajous signal only from SP, in the absence of defects, while Figures 4b-d shows Lissajous signal from OD 50% groove under SP in the three positions M1, M2 and M3, described earlier. The inspection frequency was 150 Hz. When the defect is located in position M1 and M3, its signal has higher amplitude than SP signal. However, if defect position is M2, then its signal is even smaller and it is masked by SP signal.

3 Finite Element Simulation of EDM Defects under Monju Support Plate

Finite Element simulations were conducted, using a RFEC code to validate and understand the reduction of defect signal when it is under SP. Due to the fact that all elements

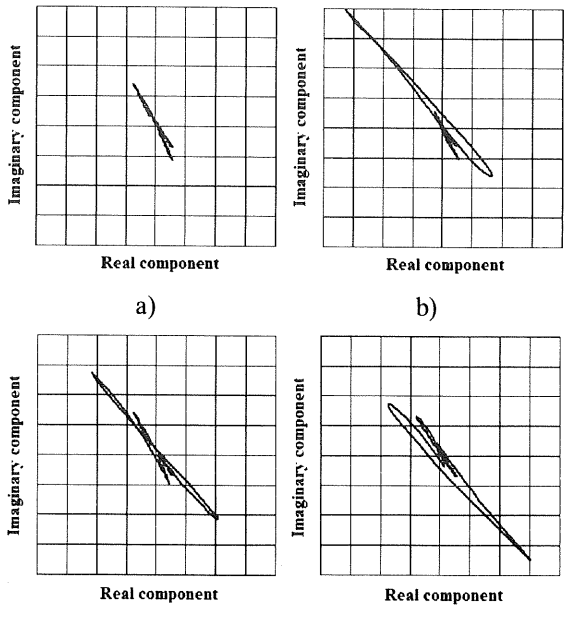

Fig 5. FEM simulation in the absence of the connection plate between the two SP legs: a) SP signal only;
SP and OD50% groove in position: b) M1; b) M2; c) M3.

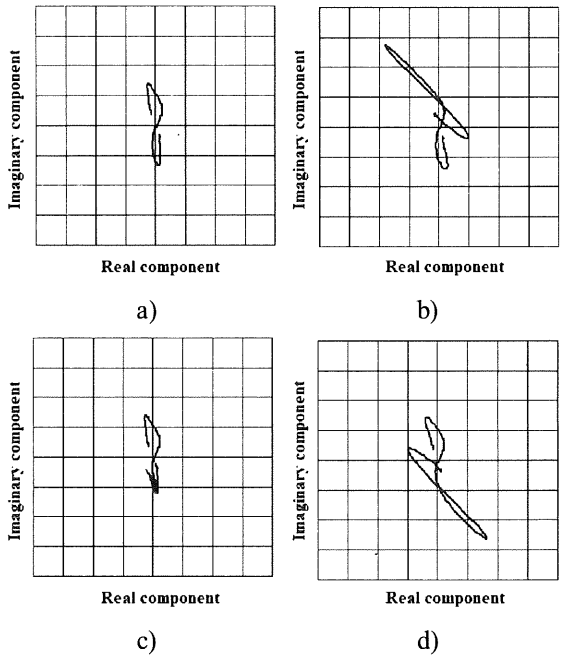

Fig.6 FEM simulation in the presence of the connection plate between the two SP legs: a) SP signal only; SP and OD50% groove in position: b) M1; b) M2; c) M3.

in the geometry, except SP, have axisymmetric properties, a 2D axisymmetric code [2] was used to simulate and calculate the RFEC signal of the detection system.

In order to find the amplification factor, used in the experimental data, the simulations results of both OD20% and OD50% groove were calibrated with experimental data. It was not needed to calibrate the phase of the signal, since the phase could be set to zero during measurements.

Both SG tube and SP are made of the same material and their electrical conductivity is 3.5×10^6 S/m while relative magnetic permeability is 95. The ring is made of austenitic stainless steel and has 1.0×10^6 S/m electrical conductivity and a relative permeability equal to 1.

The geometrical characteristics of the RFEC detection system are listed in Table 1, while tube and SP parameters are shown in Table 2.

In Figure 5a is presented a simulation of the SP signal, at 150 Hz, in the absence of the horizontal plate that connects the two SP legs. In the simulations was used the amplification factor calculated from calibration. SP signal amplitude from simulation is equal with the measured one but has a different shape. Figures 5b-d show the OD 50% groove signal, when the defect is under SP in positions M1, M2, M3. It can be seen that defect signal is higher that SP signal, when the defect is in all positions M1, M2 and M3, which is in disagreement with the experimental data from Figure 4. Also, simulated defect signal shape does not correspond to measurements. During simulations, the defect signal slightly varies due to SP, which is not true. The reason for this disagreement was caused by neglecting the effect of the plate that connects the two SP legs.

In Figure 6a is shown the simulation of SP signal, taking into account the horizontal connection plate. Figures 6b-d reveal the simulated signal from OD 50% groove under SP in position M1, M2 and M3. In all cases, simulations are very close to measurements in all aspects: amplitude, phase and signal shape.

The contour plots of the magnetic field lines are plotted in Figure 7 for both cases: absence and presence of connection plate between the two SP legs.

Table 1. Parameters of the RFEC device.

Excitation coil: inner/outer radius [mm]	7.75/9.75
Excitation coil: length [mm]	15
Excitation coil: current density [A/m^2]	10^6
Detection coil: inner/outer radius [mm]	7.75/9.75
Detection coil: number of turns	1000
Detection coil: length [mm]	5
Distance between detection coils [mm]	3
Distance excitation-detection coil [mm]	87.5

Table 2. Parameters of the SG tube and SP.

SG Tube: inner/outer radius [mm]	11.65/15.9
Ring: inner/outer1	15.9/18.4
And outer2/outer3 radius [mm]	22.5/24.5
Ring: length1/length2/length3 [mm]	8/8/6
SP (leg 1): inner1/inner2	18.4/22.5
and inner3/outer radius [mm]	24.5/31.4
SP (leg 2): inner/outer radius [mm]	18.4/31.4
SP – connection plate	19.4/29.4
inner/outer radius [mm]	
Distance between SP leg 1 - leg 2 [mm]	60
Length of SP (leg1)/ SP (leg2) [mm]	20/20

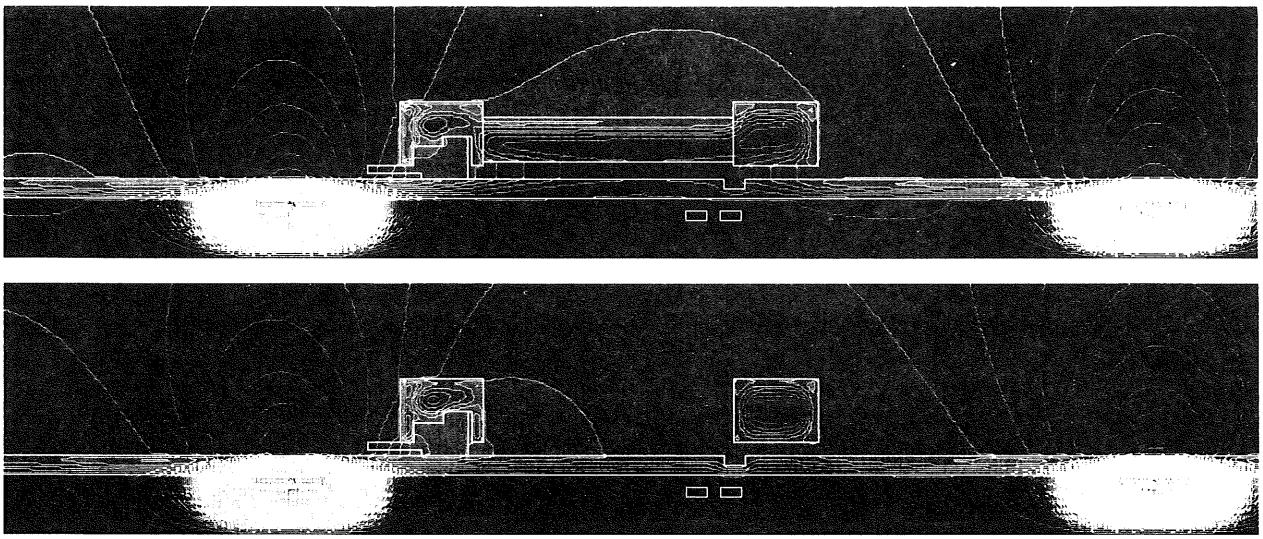

Fig. 7 Contour plots of the real part of magnetic field lines using double exciter RFEC, at 150 Hz, in the presence (upper picture) or absence (lower picture) of the horizontal SP connection plate. OD 50% groove is located under the second leg of the SP.

When the connection plate is present, the number of magnetic field lines decrease in the defect region due to the shielding effect of the plate. Most of field lines take the path through the SP. Consequently, as also was measured, the defect signal reduce its amplitude being masked by SP signal. Despite this is only a 2D axisymmetric model, it seems that the effect of the connection plate is strong enough, even if the plate is not full circumferentially.

Experimental measurements showed that if the defect is in position M2 or M3 under SP leg 2, it doesn't matter (defect signal has a similar shape) if it is on the same side with the connection plate or oppositely. Also, there is a small effect on the defect signal when SP leg 2 touch the SG tube outer surface.

4 Multi-Frequency Algorithm to Extract Defect Signal Using Experimental Data

The main difficulty in detecting a defect under SP, using RFEC system, is that the defect signal is masked by the SP signal. Using the direct measurements data even an OD50% groove, located in position M2, is difficult to be detected. The second difficulty arises from the fact that during inspection of the SG tube it is not known in advance if there is or not a defect, and if the SP leg 2 touch or not the SG tube surface.

In order to extract the defects signal, when the defect is under SP, a multi-frequency algorithm approach was considered. The RFEC system uses two frequencies in the same time, in order to record defect signal and then to subtract SP signal.

The multi-frequency algorithm is based on the assumption when eddy current frequency change there is a smaller modification of the SP signal compared with the defect signal, and that SP signal shape change linearly with the frequency.

Let's consider the shape C_1 for SP signal, at frequency ν_1 and shape C_2 for SP signal at frequency ν_2, in the absence of any defect. A simulation of SP signals, using the FEM code, is shown in the complex (X, Y) representation in Figure 8a. C2 shape is then rotated with angle α and amplified by factor k, to best fit shape C1, as is shown in Figure 8b:

$$C_1 = (x_1^i, y_1^i),\ C_2 = (x_2^i, y_2^i),\ C_3 = (x_3^i, y_3^i) \tag{1}$$

$$\begin{pmatrix} x_3^i \\ y_3^i \end{pmatrix} = k \begin{pmatrix} \cos\alpha & -\sin\alpha \\ \sin\alpha & \cos\alpha \end{pmatrix} \begin{pmatrix} x_2^i \\ y_2^i \end{pmatrix}, \quad i = 1..n$$

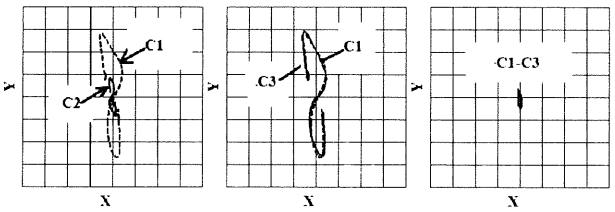

Fig. 8 FEM simulations: a) SP signal C_1 at frequency ν_1 and C_2 at frequency ν_2 b) Transformation of signal C2 to C3; c) Suppression of SP signal by subtracting C3 from C1.

In Figure 8c SP signal is suppressed by subtracting from the original C1 shape at frequency ν_1 the transformed C3 shape at frequency ν_2. The SP noise is defined as C3-C1.

Based on the accurately FEM simulations of the SP, earlier described, the main parameters of the multi-frequency algorithm were identified. First, the best two frequency set was found to be 150 and 450 Hz. At higher frequencies (more than 500 Hz), the SP signal becomes very small, the amplification factor k increases and the error in the SP subtraction consequently rise up. The SP signal amplitude has a maximum value at 150 Hz and

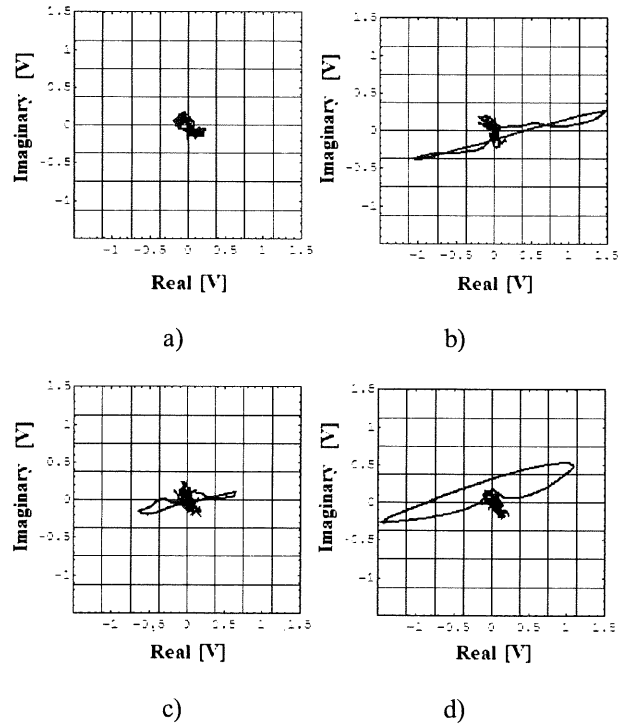

Fig. 9 Suppression of SP signal using multi-frequency algorithm and experimental data: a) SP signal; OD50% groove under SP in position: b) M1; c) M2; d) M3.

decreases for lower frequencies. Second, the values of the amplification factor k and rotation angle α were calculated once, for the particular SP geometry, SG tube characteristics and RFEC system values.

The multi-frequency algorithm was applied to the data measured for the two OD50% and OD 20% groove, when defects were located under SP in the position M1, M2 and M3. In order to reduce the noise in the data, the RFEC signal was recorded using two excitation sources in the same time with both 150 and 450 Hz frequency. At the RFEC probe moves along tube, probe vibrations add a supplementary noise in the signal, but the same noise structure will be present in both recordings at 150 and 450 Hz. Due to the subtraction technique used in the multi-frequency algorithm, this noise is also reduced.

In Figure 9a is shown the SP signal, in the absence of any defect in the SG tube, after the multi-frequency algorithm was applied to the experimental measurements and SP signal was suppressed. This signal represents only the noise and has the shape of a spot located in the graph origin point. In Figures 9b-d are shown the signal from OD50% groove under SP in position M1, M2 and M3. By applying this technique, the OD50% can be detected even if is located in position M2 (see Figure 9c), which was not previously possible using initial measurements data (presented in Figure 4c). When OD50% groove is in position M1 or M3 the defect is much more easier detected, as is shown in Figures 9b ,9d.

The main challenge in applying multi-frequency technique is to suppress not only the SP signal but also others noise (like probe wobbles and vibrations) which are correlated with the defect signal. Despite the simplicity of the method, it could better cope with the SP signal and the other noise in the signal, when experimental data were used.

5. Conclusion

Detection of EDM defects under SP of Monju FBR, in ferromagnetic SG tubes and using RFEC technique, is enhanced using a two multi-frequency algorithm to suppress the SP signal. The parameters of the multi-frequency algorithm are found out using accurate finite element simulations of the SP signal at two different frequencies.

The best frequencies set test for the particular situation, corresponding to the geometry of SG tube, SP and RFEC system were found to be 150 and 450 Hz. Outer defect 50% from tube wall thickness can be better detected using the multi-frequency algorithm, when the defect is under SP.

References

[1] D. L. Atherton, S. Sullivan and M. Daly, Br. J. Nondestructive Testing, 30, No. 1, Jan. 1988, pp. 22-28.

[2] O Mihalache, "Advanced Remote Field Computational Analysis of Steam Generators Tubes", The 8th International Workshop on Electromagnetic Nondestructive Evaluation, Saarbrucken, Germany, June 12-14, 2002.